ELSEVIER

Journal of Power Sources 81–82 (1999) 277–281

JOURNAL OF POWER SOURCES

www.elsevier.com/locate/jpowsour

Lithium intercalation in tin oxide

J. Chouvin [a,*], C. Branci [a], J. Sarradin [a], J. Olivier-Fourcade [a], J.C. Jumas [a], B. Simon [b], Ph. Biensan [b]

[a] *Laboratoire de Physicochimie de la Matière Condensée (UMR C5617 CNRS), Université Montpellier II, Place Eugène Bataillon, 34095 Montpellier Cedex5., France*

[b] *SAFT, Route de Nozay, 91460 Marcoussis, France*

Abstract

Tetragonal SnO compound was studied as the active electrode material in 'Lithium-ion'-type cell. Structural and ^{119}Sn Mössbauer properties of SnO are presented. The results concerning X-ray powder diffraction (XRD) and ^{119}Sn Mössbauer spectroscopy of lithiated crystallised tin oxide SnO between 0 and 2 lithium inserted per formula were reported. During the lithium insertion a reduction of SnO in β-Sn and in an inter-metallic tin in strong interaction with the structural SnO (SnO → β-Sn and SnO → Sn(0)) is observed. When the cell is recharged, the mechanism is in part reversible with the reformation of the SnO but there is also the formation of Sn(IV) (Sn(0) → Sn(II) → Sn(IV)).

Keywords: Tin oxide; ^{119}Sn Mössbauer; Lithium intercalation; Lithium-ion cells

1. Introduction

The perfecting of electrochemical batteries like the 'Li-ions' is actually one of priority in the lithium cells search. These batteries were characterised by a migration of lithium ions from an anode (lithium tank) towards a host structure used as cathode during the discharge and reversibly during the charge. In the commercialised 'Li-ion' cells [1], the conventional anode material is graphite [2], which can intercalate one Li per six C and allows a capacity of 327 mA h/g. Presently, efforts were made in order to improve this capacity. Recent developments by Fuji Photo Film, [3] suggest that an amorphous tin-based composite oxide can be used in the place of carbon anode. This composite offers promising electrochemical features, like for example a specific capacity of about 1200 mA h/g, but the lithium insertion mechanism into this amorphous is not well known [4,5].

In this paper, a study by ^{119}Sn Mössbauer spectroscopy and X-ray diffraction of lithiated crystallised tin oxide SnO was presented between 0 and 2 lithium inserted per formula. In the amorphous composite, this last compound is probably the active element and a study of the local environment of tin atoms during the intercalation/deintercalation can help to a better understanding of the lithium insertion process in tin oxide-based compounds.

From a structural consideration, the tin oxide has a layered structure (space group: P4/nmm) in which Sn(II) is in regular square-pyramidal coordination ($d_{Sn-O} = 2.22$ Å) [6]. The electronic structure of α-SnO shows a peak at low energy corresponding to O(s) states and a group of peaks at higher energies. In this group two peaks are due to bonding and antibonding Sn(5s)–O(p) states. Moreover, the lone pair of SnO points towards the interlayer space, creating a Van der Waals gap [7].

2. Experimental

The allotropic form α-SnO was synthesised by 'sol–gel' process [8]. A solution of 25 g of $SnCl_2,2H_2O$ in water was cleared up with hydrochloric acid and 20 g of NaOH in 200 ml of water. A white precipitate, which turned to black powder upon heating to boiling, was formed. This powder was washed by filtration and in order to crystallises the powder, an annealing at 110°C was achieved.

X-ray powder diffraction diagrams, recorded on a Philips θ-2θ diffractometer with Cu–Kα radiation ($\lambda = 1.5606$ Å), have been used in order to characterise the compounds before and after insertion of lithium into the framework. For the intercalated phases, the recording was made under

* Corresponding author

0378-7753/99/$ - see front matter
PII: S0378-7753(99)00140-8

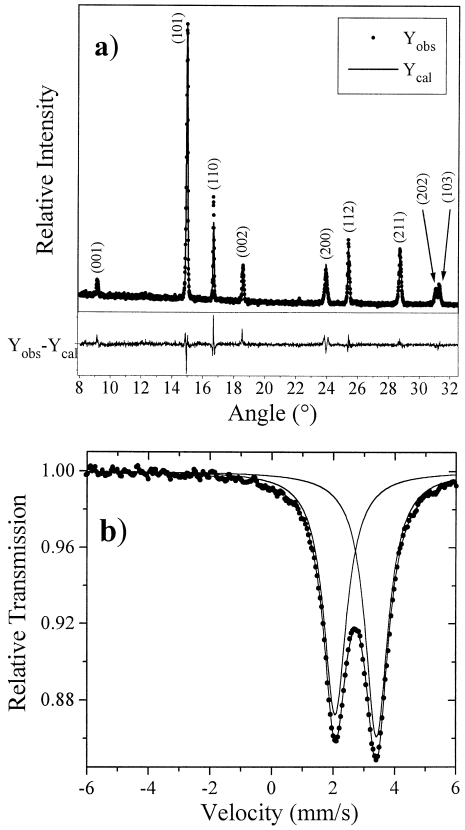

Fig. 1. (a) XRD and proposed Rietveld refinement and (b) ^{119}Sn Mössbauer spectrum of quadratic α-SnO.

vacuum in order to avoid undesirable reactions with air. Rietveld refinement of the pristine compound was carried out with the aid of a computer program DBWS-9006 developed by Wiles and Young [9].

Mössbauer spectroscopy is one of the main techniques of characterisation widely used in solid state physics and chemistry. The use of this spectroscopy here is of great interest for several reasons: (i) it completes the structural X-ray diffraction study which cannot distinguish amorphous compounds, (ii) it gives information on the electronic distribution around the tin, (iii) it follows every electronic change (oxidation state) of tin going along with insertion reactions. The spectra were measured using ELSCINT-AME40 constant acceleration spectrometer. The velocity scale was calibrated by using a ^{57}Co source and a metallic iron foil absorber. The spectra were fitted to Lorentzian profiles by least square method [10]. All isomer shifts reported here are given with respect to the centre of $BaSnO_3$ spectrum obtained with the same source.

The discharge/charge curves were carried out galvanostatically at current density of 10 mA/g between 3 and 0.8 V vs. lithium. The electrochemical cell consisted of a lithium disk (anode) and the tin oxide sample (cathode). The electrolyte was $LiPF_6$ (1 M) in PC-EC-3DMC.

Table 1
Result of Rietveld analyses of XRD data of quadratic α-SnO

	SnO	SnO
$a = b$ (Å)	3.7984 (2)	3.8029
c (Å)	4.8348 (3)	4.8382
Sn position	1/4,1/4,0.2332 (7)	2c, 1/4,1/4,0.2383
O Position	3/4,1/4,0	2a, 3/4,1/4,0
R_{Bragg}	4.74	/
S	1.6	/
Reference	This work	[6]

Table 2
Mössbauer parameters of α-SnO

	δ_{IS}	Δ_{QS}	Γ_{LW}	χ^2	Ref.
SnO	2.646 (2)	1.348 (2)	0.908	0.556	This work
SnO	2.641	1.308	/	/	[12]

δ_{IS} = isomer shift relative to $BaSnO_3$, Δ_{QS} = quadrupole splitting, Γ_{LW} = full width at half maximum. All parameters are reported in mm/s.

3. Results and discussion

3.1. The quadratic α-SnO

Black α-SnO obtained by Ditte's method [11] was examined by X-ray diffraction (XRD) (Fig. 1a) with Cu K_α radiation using a Phillips diffractometer. All nine diffraction peaks lying in the interval $8° \leq \theta \leq 32°$ were matched. The structural parameters obtained by the Rietveld analyses of the X-ray diffraction in the P4/nmm space group are summarised in Table 1. They are in good agreement with the results reported by Pannetier and Denes [6].

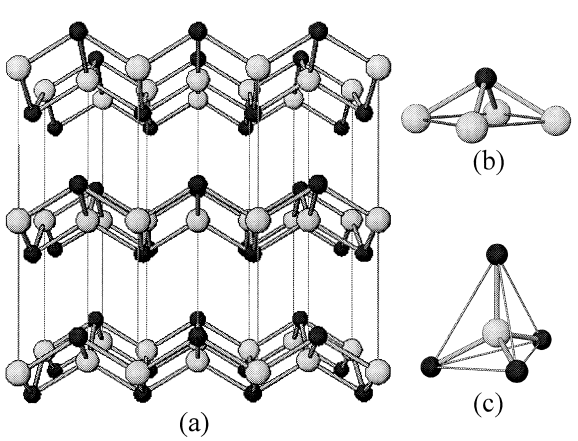

Fig. 2. (a) The crystal structure of tetragonal α-SnO; (b) the arrangement of bonds from a Sn^{2+} ion to O^{2-} and (c) the arrangement of bonds from a O^{2-} ion to Sn^{2+}.

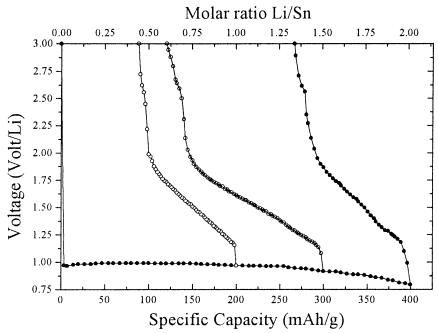

Fig. 3. Potensiostatic discharge of SnO.

Fig. 1b) shows the ^{119}Sn Mössbauer spectrum of α-SnO recorded at room temperature. The results of the fitting for SnO are given in Table 2.

The isomer shift (IS) ($\delta = 2646$ mm/s) is characteristic of the quadratic α-SnO [12]. The important value of quadrupolar shift (QS) ($\Delta = 1{,}332$ mm/s) shows a high distortion in the Sn environment. This distortion is due to the asymmetrical feature of the bonding between Sn^{2+} ion and the eight surrounding oxygen anions in the structure of α-SnO. It has a layer structure in which the tin atoms are at the apex of a square pyramid and the tin has an inert pair of electrons (Fig. 2). The main part of the asymmetry observed is due to preferred orientation in the sample, but the presence of vibrational anisotropy (Goldanskïi–Karyagin effect) cannot be discarded [13].

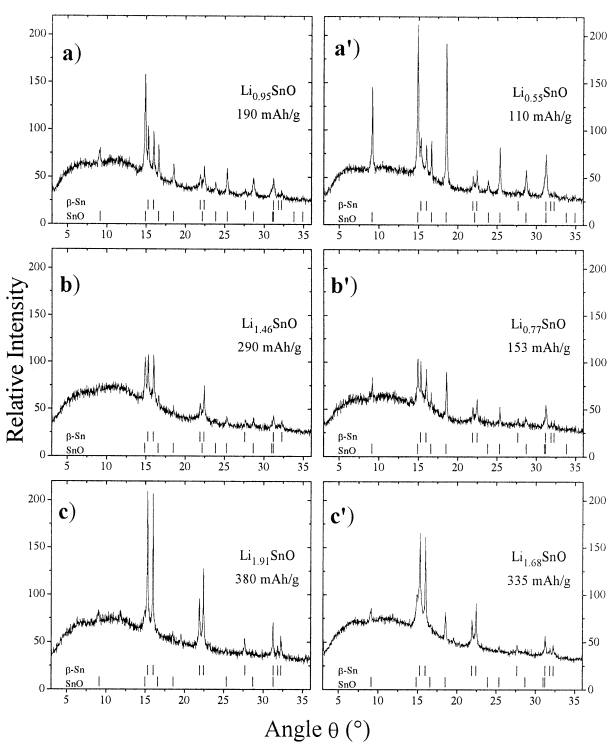

Fig. 4. XRD patterns of lithiated SnO for the charged samples at (a) 0.95 Li; (b) 1.46 Li; (c) 1.91 Li and for the discharged samples at (a′) 0.55 Li; (b′) 0.77 Li; (c′) 1.68 Li.

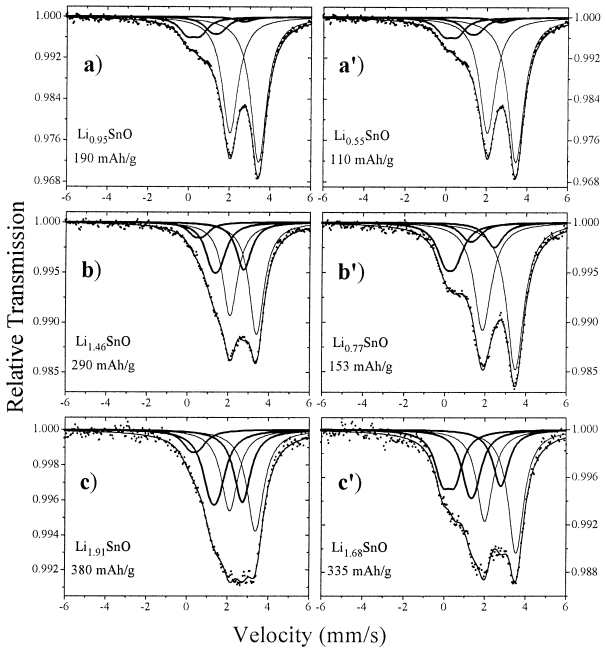

Fig. 5. ^{119}Sn Mössbauer spectra of lithiated SnO for the charged samples at (a) 0.95 Li; (b) 1.46 Li; (c) 1.91 Li and for the discharged samples at (a′) 0.55 Li; (b′) 0.77 Li; (c′) 1.68 Li.

3.2. Lithium intercalation in α-SnO

SnO was evaluated as the active electrode material in lithium anode cells. The charge–discharge capacity of SnO was examined at different states. The cell was charged to different capacities (190, 290, 380 mA h/g) and discharged to 3 V, respectively. The curves presented in Fig. 3 show the different states of intercalation for studied samples. We have to consider the possible reduction of electrolyte, which modify the number of lithium really intercalated in the framework.

Figs. 4 and 5 show, respectively, the XRD patterns and the ^{119}Sn Mössbauer spectra of the different samples. The diffraction peaks in XRD patterns (Fig. 4) was clearly

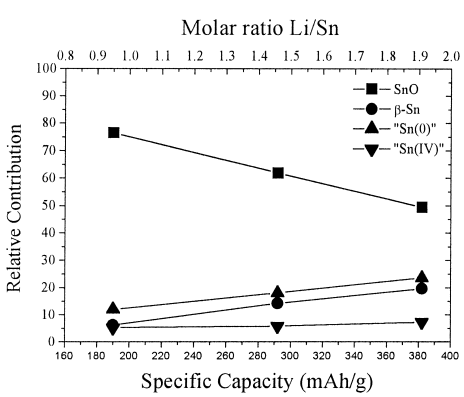

Fig. 6. Evolution of Relative Contribution, obtained by Mössbauer spectroscopy without taking into account the f factor, of different compounds during the charge of SnO.

Table 3
Hyperfine parameters of ^{119}Sn Mössbauer spectra of lithiaded SnO

	Site	δ_{IS}	Δ_{QS}	RA (%)	χ^2
Charged cells					
$Li_{0.95}SnO$ 190 mA h/g	SnO	2.649 (7)	1.351 (7)	76.51	0.463
	β-Sn	2.64 (5)		6.25	
	'Sn(0)'	1.22 (5)	0.47 (5)	11.98	
	'Sn(IV)'	0.16 (6)	0.55 (6)	5.26	
$Li_{1.46}SnO$ 290 mA h/g	SnO	2.67 (1)	1.30 (1)	61.87	0.519
	β-Sn	2.68 (2)		14.27	
	'Sn(0)'	1.29 (3)	0.38 (4)	18.03	
	'Sn(IV)'	0.45 (6)	0.44 (6)	5.83	
$Li_{1.91}SnO$ 380 mA h/g	SnO	2.65 (1)	1.26 (1)	49.43	0.474
	β-Sn	2.64 (2)		19.66	
	'Sn(0)'	1.26 (3)	0.40 (5)	23.60	
	'Sn(IV)'	0.27 (6)	0.43 (6)	7.31	
Discharged cells					
	Site	δ_{IS}	Δ_{QS}	RA (%)	χ_2
$Li_{0.55}SnO$ 110 mA h/g	SnO	2.649 (5)	1.405 (5)	82.42	0.814
	β-Sn	2.63 (5)		1.57	
	'Sn(0)'	1.24 (5)	0.43 (5)	6.66	
	'Sn(IV)'	0.14 (5)	0.63 (5)	9.35	
$Li_{0.77}SnO$ 153 mA h/g	SnO	2.59 (2)	1.61 (2)	70.55	0.617
	β-Sn	2.34 (7)		6.85	
	'Sn(0)'	1.19 (8)	0.36 (7)	5.96	
	'Sn(IV)'	0.17 (5)	0.50 (6)	16.64	
$Li_{1.68}SnO$ 335 mA h/g	SnO	2.67 (2)	1.54 (2)	49.77	0.551
	β-Sn	2.69 (3)		13.09	
	'Sn(0)'	1.25 (3)	0.31 (3)	17.64	
	'Sn(IV)'	0.13 (4)	0.61 (4)	19.50	

identified. Indeed, they are two different compounds: SnO and β-Sn. This observation allows to fit the ^{119}Sn Mössbauer spectra with two subspectra relative to SnO and β-Sn. In the XRD and ^{119}Sn Mössbauer spectra, we can observe the decrease of the SnO proportion and the increase of the β-Sn proportion when the capacity is higher (Fig. 4a,b,c,Fig. 5a,b,c). This can be interpreted by the reduction $Sn^{2+} + 2e^- \rightarrow Sn^0$ during intercalation of lithium in the material. When each sample is recharged (Fig. 4a′,b′,c′ Fig. 5a′,b′,c′), we have the opposite evolution which corresponds to the partial oxidation $Sn^0 \rightarrow Sn^{2+} + 2e^-$ when lithium is released. The capacity dependence of the area under the resonance lines for different compounds is shown in Fig. 6. The areas are in relative percentages. A good linearity in their variation can be observed.

However, the difference in the proportion of β-Sn obtained by XRD and Mössbauer spectroscopy is due to the weak value of the Mössbauer recoilless fraction (f factor) in β-Sn at room temperature. Indeed, at 300 K, we have f(β-Sn) = 0.045 [14] when f(SnO) = 0.35 [13].

On the other hand, the Mössbauer spectra, in relation to XRD patterns, have two more contributions necessary to fit correctly the spectra (Table 3). The first ($\delta = 0.16 - 0.45$ mm/s and $\Delta = 0.43 - 0.55$ mm/s) can be attributed to Sn(IV) oxide, due to an accidental oxidation during manipulation and measurement. The second ($\delta = 1.22 - 1.29$ mm/s and $\Delta = 0.38 - 0.47$ mm/s) is representative of a Sn(0) in strong interaction with the structural SnO. This tin is like tin in PtSn alloys formed during the reduction of bimetallic catalysts Pt–Sn/Al_2O_4 and with an isomeric shift between 1.2–1.5 mm/s [15]. Its contribution increases linearly with the capacity for the charged samples. When each sample is discharged, the part of this Sn(0) decrease significantly. That shows this contribution has an important role in the mechanism of intercalation/de-intercalation of lithium in SnO.

Concerning the evolution of the specific capacity vs. relative contribution (Fig. 6), the unknown value of the f factor corresponding to this Sn(0) will not allow to obtain the absolute value of the relative contribution.

The Sn(IV) contribution is constant for the different discharged samples (5%), while it amplifies when the cells are discharged and the increase is more and more important when the insertion is higher. The fact that we obtained Sn(IV) shows that the mechanism is not completely reversible since we obtained Sn(IV) instead of Sn(II) during the discharge of the cell. We have a complex mechanism of oxidation Sn(0) → Sn(II) → Sn(IV) when the lithium is de-intercalated from tin oxide.

4. Conclusion

The results of the intercalation/de-intercalation of lithium between 0 and 2 lithium in crystallised SnO have shown a complex mechanism of oxido-reduction. For the charge of SnO (lithium intercalation), to two lithium, the XRD related to ^{119}Sn Mössbauer spectroscopy bring out a mechanism of reduction in two steps with the simultaneous reduction SnO → β-Sn and SnO → Sn(0), where Sn(0) is an inter-metallic tin in strong interaction with the structural SnO. During the charge, we have an interesting feature: the reformation of SnO. Furthermore, the oxidation mechanism has another step: the complex and simultaneous oxidation of tin atoms: Sn(0) → Sn(II) → Sn(IV). So, the intercalation/de-intercalation of lithium in crystallised tin oxide is carried out by a complex mechanism of oxido-reduction. However, some study of ^{119}Sn Mössbauer spectroscopy for more than two lithium inserted per formula are actually in progress in order to confirm the presence or not of Li–Sn alloys found by Courtney and Dahn [4]. Moreover, the study of lithium insertion into amorphous tin-based composite oxide is also in progress.

References

[1] Sony Lithium Ion Battery Performance Summary, JEC Batt., Vol. 2, 1994, p. 31.
[2] J.R. Dahn, T. Zheng, Y. Liu, J.S. Xue, Science 270 (1995) 590.
[3] Fuji Photo Film, European patent, EP 0 704 921 A1, 1995.
[4] I.A. Courtney, J.R. Dahn, J. Electrochem. Soc. 144 (1997) 2045.
[5] Y. Iodata, T. Kubota, A. Matsufuji, Y. Maekawa, T. Miyasaka, Science 276 (1997) 1385.

[6] J. Pannetier, G. Denes, Acta. Cryst. B 36 (1980) 2763.
[7] I. Lefebvre, M.A. Szymanski, J. Olivier-Fourcade, J.C. Jumas, Phys. Rev. B 58 (4) (1998) 1896.
[8] B. Harry, B. Weiser, O. Milligan, J. Phys. Chem. 36 (1932) 3039.
[9] D.B. Wiles, R.A. Young, J. Appl. Crystallogr. 28 (1995) 366.
[10] W. Kündig, Nucl. Instrum. Methods 75 (1969) 336.
[11] H.B. Weiser, W.O. Milligan, J. Phys. Chem. 36 (1932) 3039.
[12] R.H. Herber, Phys. Rev. B 27 (1983) 4013.
[13] M.S. Moreno, R.C. Mercader, Phys. Rev. B 50 (1994) 9875.
[14] A.A. Bakgat, Phys. Stat. Sol. B 97 (1980) K129.
[15] M.C. Hobson Jr., S.L. Goresh, G.P. Khare, J. Catal. 142 (1993) 641.